# Models for Nucleoside Glycosylase Enzymes. Evidence That the Hydrolysis of β-D-Ribofuranosides Requires a "Backside" Preassociation Nucleophile

**Xavier M. Cherian, Scott A. Van Arman, and Anthony W. Czarnik***

*Contribution from the Department of Chemistry, The Ohio State University, Columbus, Ohio 43210.* *Received August 14, 1989*

**Abstract:** We have compared the pH-independent rates of glycosidic hydrolysis in a series of four fluorenone ketal derivatives of *p*-nitrophenyl β-D-ribofuranoside with each other and with that of *p*-nitrophenyl β-D-ribofuranoside itself. A syn-oriented carboxylate group clearly affords catalysis in the reaction and is more effective than identically oriented amide and ester groups by factors of at least 100- and 240-fold, respectively. The effect of the carboxylate can be viewed in three different ways: it provides a 3.2-fold acceleration as compared to underivatized *p*-nitrophenyl β-D-ribofuranoside, an approximately 30-fold acceleration when the decelerating effect of the ketal group is considered, and an 860-fold acceleration as compared to the compound that models an Asp-52 → Ala-52 mutant lysozyme. Most strikingly, the hydrolysis of a reference compound with impeded backside solvation of the oxocarbonium ion is very slow and provides a direct experimental verification for the importance of backside solvent participation in the hydrolysis reaction of a nucleoside analogue. These kinetic results do not provide any evidence concerning two potential explanations for the role of carboxylate in acetal hydrolysis: electrostatic destabilization of the ES complex by binding-induced desolvation of the carboxylate ion and lone pair exchange repulsion. The results are consistent with two other proposed carboxylate roles: electrostatic stabilization of an oxocarbonium ion like transition structure and anchimeric assistance by the carboxylate. While the most likely role for carboxylate in acetal hydrolysis is as a nucleophile, the low reactivity of the *endo*-amide and the unexceptional reactivity of the syn-oriented *endo*-carboxylate more directly support the electrostatic stabilization mechanism for the hydrolyses of these riboside derivatives.

Glycosidic hydrolysis (also called glycolysis, depurination) of purine nucleosides is a fundamental process in the chemistry of DNA both in vivo (Scheme I) and in vitro. Glycosidic hydrolysis of intrastrand nucleotides yields AP sites, which have recently been characterized by Gerlt using $^{13}C$ NMR;[1] in addition, Gerlt has studied the chemical mechanism by which UV endonuclease V excises AP sites in DNA.[2] The principal biological effect of such AP site forming mutations is error-prone DNA synthesis;[3-6] it has been reported that T4 DNA polymerase, DNA polymerase I, AMV reverse transcriptase, and DNA polymerase α all stop at AP sites.[7] Consequently, the study of DNA glycosylase mechanisms remains an active area of investigation. Activities and mechanisms continue to be elucidated for enzymes that effect glycosyl transfers of nucleoside derivatives such as hypoxanthine,[8] AMP,[9] ADP-ribose from NAD,[10] the intrastrand thymine dimer,[11] and 5,6-dihydroxy-5,6-dihydrothymine.[12] Glycosylases such as uridine phosphorylase, thymidine phosphorylase, and purine nucleoside phosphorylase have been used extensively by Krenitsky and Rideout for the facile synthesis of unnatural nucleoside derivatives.[13]

While little is known about the detailed chemical mechanism of glycosylase section, mechanistic studies on acid-catalyzed purine

**Scheme I**

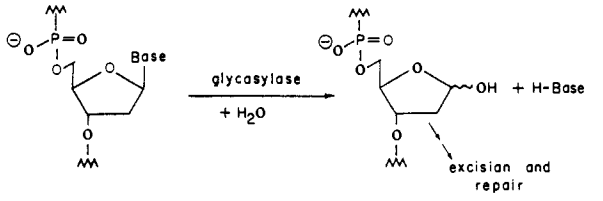


**Scheme II**

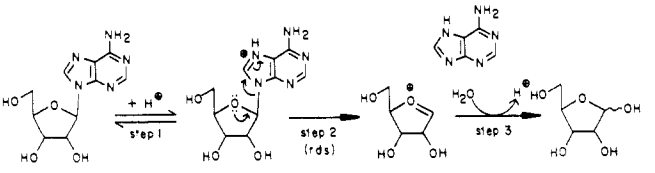


nucleoside glycolysis firmly establish a pathway involving (1) protonation of the nucleic acid base, (2) rate-limiting heterolytic cleavage of the glycosidic linkage, and (3) rapid addition of water (Scheme II).[14-22] The kinetic effects of adenosine sugar ring modification[18,23] and of base methylation[18,24] on the rate of depurination have been reported, as have the effects of guanosine methylation[25,26] and of benzylation at N-7 with electron-with-

(1) Manoharan, M.; Ransom, S. C.; Mazumder, A.; Gerlt, J. A.; Wilde, J. A.; Withka, J. A.; Bolton, P. H. *J. Am. Chem. Soc.* **1988**, *110*, 1620.
(2) Manoharan, M.; Mazumder, A.; Ransom, S. C.; Gerlt, J. A.; Bolton, P. H. *J. Am. Chem. Soc.* **1988**, *110*, 2690.
(3) Schaaper, R. M.; Load, L. A. *Proc. Natl. Acad. Sci. U.S.A.* **1981**, *78*, 1773.
(4) Schaaper, R. M.; Glickman, B. W. *MGG, Mol. Gen. Genet.* **1982**, *185*, 404.
(5) Schaaper, R. M.; Glickman, B. W.; Loeb, L. A. *Mutat. Res.* **1982**, *106*, 1.
(6) Kunkel, T. A.; Schaaper, R. M.; Loab, L. A. *Biochemistry* **1983**, *22*, 2378.
(7) Sagher, D.; Strauss, B. *Biochemistry* **1983**, *22*, 4518.
(8) Syed, D. B.; Strauss, R. S.; Sloan, D. L. *Biochemistry* **1987**, *26*, 1051.
(9) DeWolf, W. E., Jr.; Emig, F. A.; Schramm, V. L. *Biochemistry* **1986**, *25*, 4132.
(10) Osborne, J. C., Jr.; Stanley, S. J.; Moss, J. *Biochemistry* **1985**, *24*, 5235.
(11) Liuzzi, M.; Weinfeld, M.; Paterson, M. C. *Biochemistry* **1987**, *26*, 3315.
(12) Higgins, S. A.; Frenkel, K.; Cummings, A.; Teebor, G. W. *Biochemistry* **1987**, *26*, 1683.
(13) For example, see: Krenitsky, T. A.; Rideout, J. L.; Chao, E. Y.; Koszalka, G. W.; Gurney, F.; Crouch, R. C.; Cohn, N. K.; Wolberg, G.; Vinegar, R. *J. Med. Chem.* **1986**, *29*, 138.
(14) Zoltewicz, J. A.; Clark, D. F.; Sharpless, T. W.; Grahe, G. *J. Am. Chem. Soc.* **1970**, *92*, 1741.
(15) Brown, D. M. In *Basic Principles in Nucleic Acid Chemistry*; Ts'o, P. O. P., Ed.; Academic Press: New York, 1974; Vol. II, Chapter 1.
(16) Walker, R. T. *Annu. Rep. Prog. Chem.* **1972**, *69B*, 531.
(17) Romero, R.; Stein, R.; Bull, H. G.; Cordes, E. H. *J. Am. Chem. Soc.* **1978**, *100*, 7620.
(18) Garrett, E. R.; Mehta, P. J. *J. Am. Chem. Soc.* **1972**, *94*, 8532.
(19) Parkin, D. W.; Leung, H. B.; Schramm, V. L. *J. Biol. Chem.* **1984**, *259*, 9411.
(20) Cordes, E. H.; Bull, H. G. In *Transition States of Biochemical Processes*; Gandour, R. D., Schowen, R. L., Eds.; Plenum Press: New York, 1978; pp 429-465 (especially pp 456-458).
(21) Zoltewicz, J. A.; Clark, D. F. *J. Org. Chem.* **1972**, *37*, 1193.
(22) Panzica, R. P.; Rousseau, R. J.; Robins, R. K.; Townsend, L. B. *J. Am. Chem. Soc.* **1972**, *94*, 4708.
(23) York, J. L. *J. Org. Chem.* **1981**, *46*, 2171.
(24) Saito, T.; Fujii, T. *J. Chem. Soc., Chem. Commun.* **1979**, 135.
(25) Lawley, P. D.; Brookes, P. *Biochem. J.* **1963**, *89*, 127.
(26) (a) Margison, G. P.; O'Connor, P. J. *Biochim. Biophys. Acta* **1973**, *331*, 349. (b) Singer, B. *Biochemistry* **1972**, *11*, 3939.

0002-7863/90/1512-4490$02.50/0 © 1990 American Chemical Society

drawing and -donating benzyl groups.[27] Oppenheimer has shown that the accelerated glycosidic hydrolysis of $NAD^+$ under strongly basic conditions results from deprotonation of the 2′-hydroxyl group.[28] Schramm has described a complete kinetic isotope study of both the acid- and nucleosidase-catalyzed glycosidic hydrolyses of 5′-AMP and concludes that an $S_N1$ mechanism is operative in both reactions.[29]

Physical–organic studies of the hydrolysis of aldopyranosides, while not rigorously comparable to that of aldofuranosides, may be of relevance to a study of hydrolysis in ribofuranosides. In a study designed to test the validity of "stereoelectronic control" of glycosidic hydrolysis, Sinnott has concluded that the reactions of aldopyranosyl derivatives in water are truly $S_N1$ reactions, with no preassociation of the ultimate nucleophile.[30] Of course, this does not speak directly to the mechanism of enzyme-catalyzed glycosidic hydrolysis such as that catalyzed by lysozyme, which has rather firmly been held to induce cleavage of its substrate's exocyclic oxygen. Quite recently, the idea of endocyclic cleavage has resurfaced in a proposal by Karplus, based on molecular dynamics simulations of the enzyme–substrate complex.[31a] Experimental evidence that the hydrolysis of tetrahydropyranyl acetals occurs via both exo- and endocyclic cleavage has been reported by Franck, in which the intermediate oxocarbonium ions are trapped by an intramolecular nucleophile.[31b] It is noteworthy that an aldofuranoside, 2-propyl α-arabinofuranoside, has also been shown to hydrolyze via endocyclic cleavage.[32] However, the evidence in sum still suggests that nucleosides, methylated nucleosides, and ribosides with strongly electron-deficient aglycons hydrolyze by an "$S_N1$-like" mechanism with exocyclic cleavage in the specific-acid-mediated pathway.

As nucleoside glycosylases accomplish the same general transformation as does lysozyme, and given our observation that at least one nucleoside glycosylase (PNPase) utilizes a *p*-nitrophenyl riboside as a substrate,[78] it is reasonable to think of nucleoside glycosylase activity in the light of chemical models for lysozyme action.[33] The function of lysozyme's Glu-35 as a general acid catalyst has been extensively modeled; rate enhancements as high as $10^6$ have been reported.[33b,34,35] Hogg has shown by proton inventory investigation that the hydrolysis of a simple acylal model for a possible lysozyme–substrate covalent intermediate may occur via three distinct specific-acid-catalyzed pathways.[36] There seems, therefore, to be a plethora of well-modeled, productive mechanisms by which acids may catalyze acetal hydrolysis.

Likewise, there have been several different proposals for ways in which an adjacent carboxylate ion, modeling the function of lysozyme's Asp-52 residue, might accelerate acetal hydrolysis. (1) Electrostatic stabilization of an oxonium ion like transition structure. Electrostatic stabilization of an oxocarbonium ion intermediate was proposed by Phillips after his group's solution of the lysozyme crystal structure revealed the presence of Asp-52.[37]

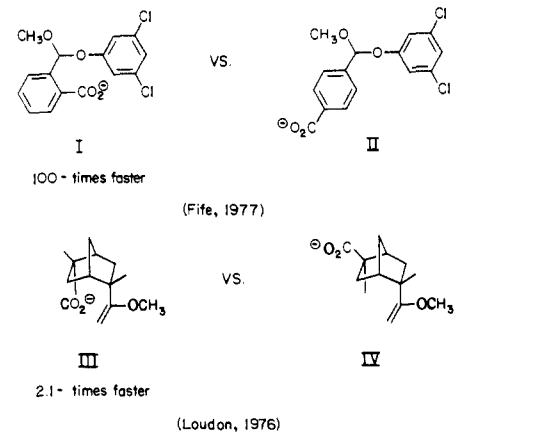


**Figure 1.** Some enzyme model compounds examined previously to test the role of carboxylate catalysis in acetal hydrolysis.

Computational studies by Warshel and Levitt[38] and Scheraga[39] of the complete lysozyme–substrate complex together with the surrounding solvent deemphasize the significance of closed-shell (steric) strain in the energetics of lysozyme catalysis. However, the importance of electrostatic stabilization of the transition state by an interaction with Asp-52 was strongly indicated. (2) Anchimeric assistance. While kinetic isotope studies of the lysozyme reaction have been interpreted previously to indicate the formation of an oxocarbonium ion by an $S_N1$ mechanism, it has more recently been shown that acetal hydrolysis involves an "exploded" transition structure that would not give kinetic isotope data consistent with $S_N1$ or $S_N2$ mechanistic extremes.[40] Therefore, the kinetically indistinguishable mechanism of anchimeric assistance by Asp-52 remains a likely possibility. (3) Electrostatic destabilization of the ES complex by binding-induced desolvation of the carboxylate ion. The active site of lysozyme, hydrated in free solution, is partially dehydrated upon binding to an oligosaccharide.[41,42] Computational studies[38,39,43–45] have supported the idea proposed by Vernon[46] that ground-state desolvation of Asp-52 could result in reactant destabilization, affording a driving force for catalysis that has been referred to as "electrostatic strain".[38] It is significant that Cordes has reported evidence for strain in the action of purine nucleoside phosphorylase without detailing the origin of this effect.[47] (4) Lone pair exchange repulsion. We have proposed that a binding-induced repulsion between nonbonded electrons on the carboxylate and carbohydrate ring oxygens would destabilize the acetal region via a point repulsive interaction that is increased as the transition structure is approached.[48] Kirby has put forward this view in a slightly different way, by noting that the ring oxygen is expected to be in a negative environment, raising the donor capability of the lone pairs.[49] A crystal structure–reactivity correlation for the hydrolysis of various pyranosides has been reported by the same author, indicating that acetals with elongated exocyclic C–O bonds (as predicted computationally to occur during lone pair exchange repulsion)[48] indeed undergo hydrolysis more quickly.[50]

(27) Moschel, R. C.; Hudgins, W. R.; Dipple, A. *J. Org. Chem.* **1984**, *49*, 363.
(28) Johnson, R. W.; Marschner, T. M.; Oppenheimer, N. J. *J. Am. Chem. Soc.* **1988**, *110*, 2257.
(29) Parkin, D. W.; Schramm, V. L. *Biochemistry* **1987**, *26*, 913.
(30) Bennet, A. J.; Sinnott, M. L. *J. Am. Chem. Soc.* **1986**, *108*, 7287.
(31) (a) Post, C. G.; Karplus, M. *J. Am. Chem. Soc.* **1986**, *108*, 1317. (b) Gupta, R. B.; Franck, R. W. *J. Am. Chem. Soc.* **1987**, *109*, 6554.
(32) Lonnberg, H.; Kulonpaa, A. *Acta Chem. Scand., Ser. A* **1977**, *31*, 306.
(33) For reviews of lysozyme model chemistry, see: (a) Chipman, D. M.; Sharon, N. *Science* **1969**, *165*, 454. (b) Kirby, A. J. *CRC Crit. Rev. Biochem.* **1987**, *22*, 283. (c) Sinnott, M. L. In *Enzyme Mechanisms*; Page, M. I., Williams, A., Eds.; Royal Society of Chemistry, Burlington House: London, 1987; p 259. (d) Czarnik, A. W. Intramolecularity: Proximity and Strain. In *Molecular Structure and Energetics, Vol. 9: Principles of Enzyme Activity*; Liebman, J. F., Greenberg, A., Eds.; VCH Publishers: New York, 1988; pp 75–117.
(34) Cordes, E. H.; Bull, H. G. *Chem. Rev.* **1974**, *74*, 581 (especially pp 599–602).
(35) For a summary of work by several labs on general-acid catalysis in acetal hydrolysis, see: Sinnott, M. I. In *The Chemistry of Enzyme Action*; Page, M. I., Ed.; Elsevier: Amsterdam, 1984; pp 417–420.
(36) Bokser, A. D.; York, K. A.; Hogg, J. L. *J. Org. Chem.* **1986**, *51*, 92.
(37) Blake, C. C. F.; Mair, G. A.; North, A. C. T.; Phillips, D. C.; Sarma, V. R. *Proc. R. Soc. London, B* **1967**, *167*, 365.
(38) Warshel, A.; Levitt, M. *J. Mol. Biol.* **1976**, *103*, 227.
(39) For a review of work on this topic, see: Pincus, M. R.; Scheraga, H. A. *Acc. Chem. Res.* **1981**, *14*, 299.
(40) See pp 293–294 and refs 57–60 of ref 33b.
(41) Kelly, J. A.; Sielcki, A. R.; Sykes, B. D.; James, M. N. G.; Phillips, D. C. *Nature* **1979**, *282*, 875.
(42) Ford, L. O.; Johnson, L. N.; Machin, P. A.; Philips, D. C.; Tjian, R. *J. Mol. Biol.* **1974**, *88*, 349.
(43) Levitt, M. Quoted in ref 42.
(44) Warshel, A. In *Peptides: Proceedings of the 5th American Peptide Symposium*; Goodman, M., Meienhofer, J., Eds.; Halsted Press: New York, 1977; p 574.
(45) Warshel, A. *Pontif. Acad. Sci. Scr. Varia* **1984**, *55*, 59.
(46) Vernon, C. A. *Proc. R. Soc. London, B* **1967**, *167*, 389.
(47) Stein, R. L.; Romero, R.; Bull, H. G.; Cordes, E. H. *J. Am. Chem. Soc.* **1978**, *100*, 6249.
(48) Bakthavachalam, V.; Czarnik, A. W. *Tetrahedron Lett.* **1987**, *28*, 2925.
(49) See ref 33b, p 308.

**Scheme III**

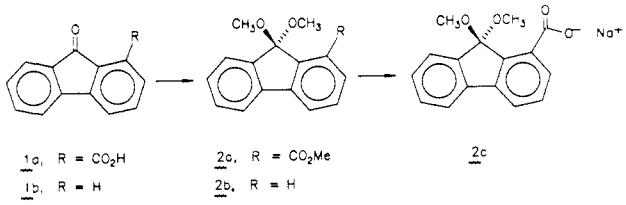

1a, R = $CO_2H$ 2a, R = $CO_2Me$ 2c
1b, R = H 2b, R = H

However, the acceleration of acetal hydrolysis afforded by intramolecular carboxylate[51-54] groups in model systems is much less pronounced than that seen by intramolecular general acids.[55] For example, the hydrolysis of *o*-carboxylate **I** (Figure 1) is 100 times faster in the pH-independent region than that of the corresponding para isomer II as reported by Fife.[53] In this model compound, it is not possible to distinguish between electrostatic stabilization of an oxocarbonium ion by the carboxylate and direct anchimeric participation by attack on the acetal, although the author prefers the first explanation. While there is by no means agreement on this point, lysozyme itself has been suggested to involve formation of an oxocarbonium ion intermediate (every major textbook depicts lysozyme's mechanism in this way); it is therefore of interest to differentiate between these mechanistic possibilities. Toward this end, Loudon has described the study of norbornane-based models III and IV (Figure 1), in which the carboxylate may serve to accelerate the general-acid-catalyzed vinyl ether hydrolysis only via electrostatic stabilization of the oxocarbonium ion (anchimeric assistance is prohibited for geometric reasons). In this elegant piece of work, much synthesis effort was expended to provide a highly useful result: *endo*-carboxylate **III** affords a 2-fold acceleration as compared to *exo*-carboxylate IV.[56] Thus, it is well established that at best carboxylate does no better a job of electrostatically stabilizing an adjacent oxocarbonium ion than does bulk water.

In 1981, Gandour noted that the syn-oriented carboxylates found at enzyme active sites should be both more basic (by $>10^4$) and, presumably, more nucleophilic than the anti-oriented carboxylates utilized in enzyme models.[57] Several groups have recently described the synthesis and evaluation of enzyme models of proton transfer using syn-oriented carboxylate bases.[58] Thermodynamic and kinetic basicity effects have consistently hovered near a 10-fold enhancement; computational analyses by Houk have attributed the lack of large increases in reported systems to hydrogen-bonding and approach-angle effects.[59] In this paper, we report our studies on riboside-based nucleoside glycosidase models **4**, **6**, **7**, and **9**, in which the "stereoelectronically correct" syn orientation of functional groups is required for geometric reasons.[60]

## Results

**Synthesis.** Fluorenone ketal **2a** was prepared by the acid-catalyzed reaction of the known 1-carboxyfluorenone (**1a**)[61] with methanol and trimethyl orthoformate, which effected the esterification and ketalization reactions in one step (Scheme III). While this reaction afforded only a 52% yield even after optimization of the conditions, another 40% of the fluorenone ester (**1**, R = $CO_2Me$) was obtained as well, indicating the ready reversibility of this ketal-forming reaction even under conditions that should have given nearly quantitative conversions. Ketalization of fluorenone (**1b**), which served as a reference compound, was similarly accomplished to give **2b**. Hydrolysis of **2a** in methanolic NaOH afforded the crystalline sodium salt **2c** in analytically pure form. Isolation of the salt in this way avoided the need for extraction of the free acid of **2c**, which could not be accomplished without significant hydrolysis to **1a**.

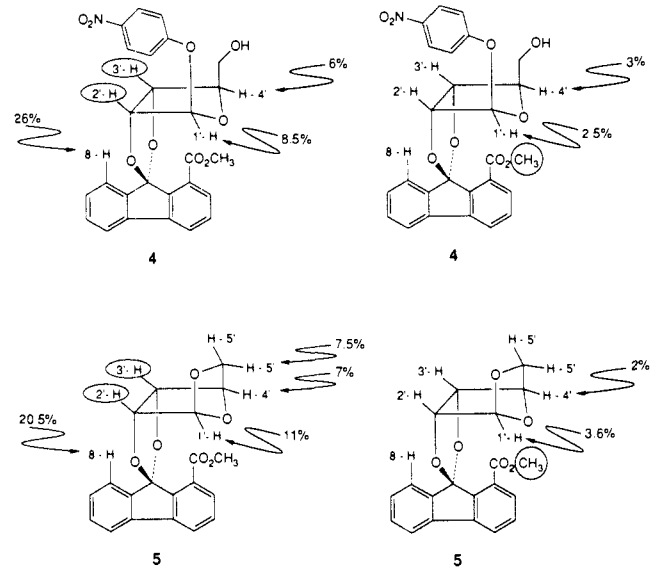

**Figure 2.** The % NOE observed in each compound upon irradiation of the circled proton(s).

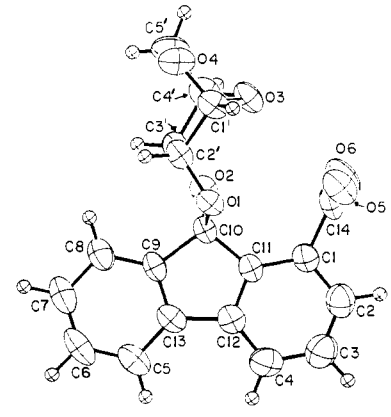

**Figure 3.** X-ray structure of the anhydrous *endo*-carboxylate **8**.

As shown in Scheme IV, reaction of the known *p*-nitrophenyl ribofuranoside (**3**)[62] with ketal **2a** afforded a mixture of **4** (25%, based on unrecovered starting material) and **5** (4%), together with several nonspiro ketals (i.e., one methyl group of the ketal remained). Acid-catalyzed conversion of **4** to **5** proceeded cleanly. The only spiro ketals observed in both reactions had the endo stereochemistry shown; attempts to observe even small amounts of exo isomer formation by NMR of the crude reaction mixtures were totally unsuccessful. A rationalization for the stereoselectivity observed in this spiroketalization reaction is given under Discussion and Conclusions. Stereochemical assignments were made both on the basis of NOE interactions (summarized in Figure 2) and on the results of an X-ray structure determination for **8** (Figure 3).

Basic hydrolysis of ester **4** provided the carboxylate form of **6**; extraction of acid **6** from aqueous acid was successful, providing

(50) (a) Allen, F. H.; Kirby, A. J. *J. Am. Chem. Soc.* **1984**, *106*, 6197. See also: (b) Edwards, M. R.; Jones, P. G.; Kirby, A. J. *J. Am. Chem. Soc.* **1986**, *108*, 7067.
(51) Capon, B.; Page, M. I. *J. Chem. Soc., Perkin Trans. 2* **1972**, 2057.
(52) Anderson, E.; Fife, T. H. *J. Am. Chem. Soc.* **1973**, *95*, 6437.
(53) Fife, T. H.; Przystas, T. J. *J. Am. Chem. Soc.* **1977**, *99*, 6693.
(54) Fife, T. H.; Pryzstas, T. J. *J. Am. Chem. Soc.* **1979**, *101*, 1202.
(55) Anchimeric assistance by intramolecular acetamido groups has been shown to provide much larger rate increases: Piszkiewicz, D.; Bruice, T. C. *J. Am. Chem. Soc.* **1968**, *90*, 2156.
(56) Loudon, G. M.; Smith, C. K.; Zimmerman, S. E. *J. Am. Chem. Soc.* **1974**, *96*, 465.
(57) Gandour, R. D. *Bioorg. Chem.* **1981**, *10*, 169.
(58) (a) Zimmerman, S. C.; Cramer, K. D. *J. Am. Chem. Soc.* **1988**, *110*, 5906. (b) Huff, J. B.; Askew, B.; Duff, R. J.; Rebek, J., Jr. *J. Am. Chem. Soc.* **1988**, *110*, 5908. (c) Lindsey, J. S.; Kearney, P. C.; Duff, R. J.; Tjivikua, P. T.; Rebek, J., Jr. *J. Am. Chem. Soc.* **1988**, *110*, 6575. (d) Tadayoni, B. M.; Parris, K.; Rebek, J., Jr. *J. Am. Chem. Soc.* **1989**, *111*, 4503.
(59) Li, Y.; Houk, K. N. *J. Am. Chem. Soc.* **1989**, *111*, 4505.
(60) Some of the work described in this paper has been communicated previously in abbreviated form: Cherian, X. M.; Van Arman, S. A.; Czarnik, A. W. *J. Am. Chem. Soc.* **1988**, *110*, 6566.
(61) Fieser, L. F.; Seligman, A. M. *J. Am. Chem. Soc.* **1935**, *57*, 2174.
(62) Honma, K.; Nakazima, K.; Uematsu, T.; Hamada, A. *Chem. Pharm. Bull.* **1976**, *24*, 394.

**Scheme IV**

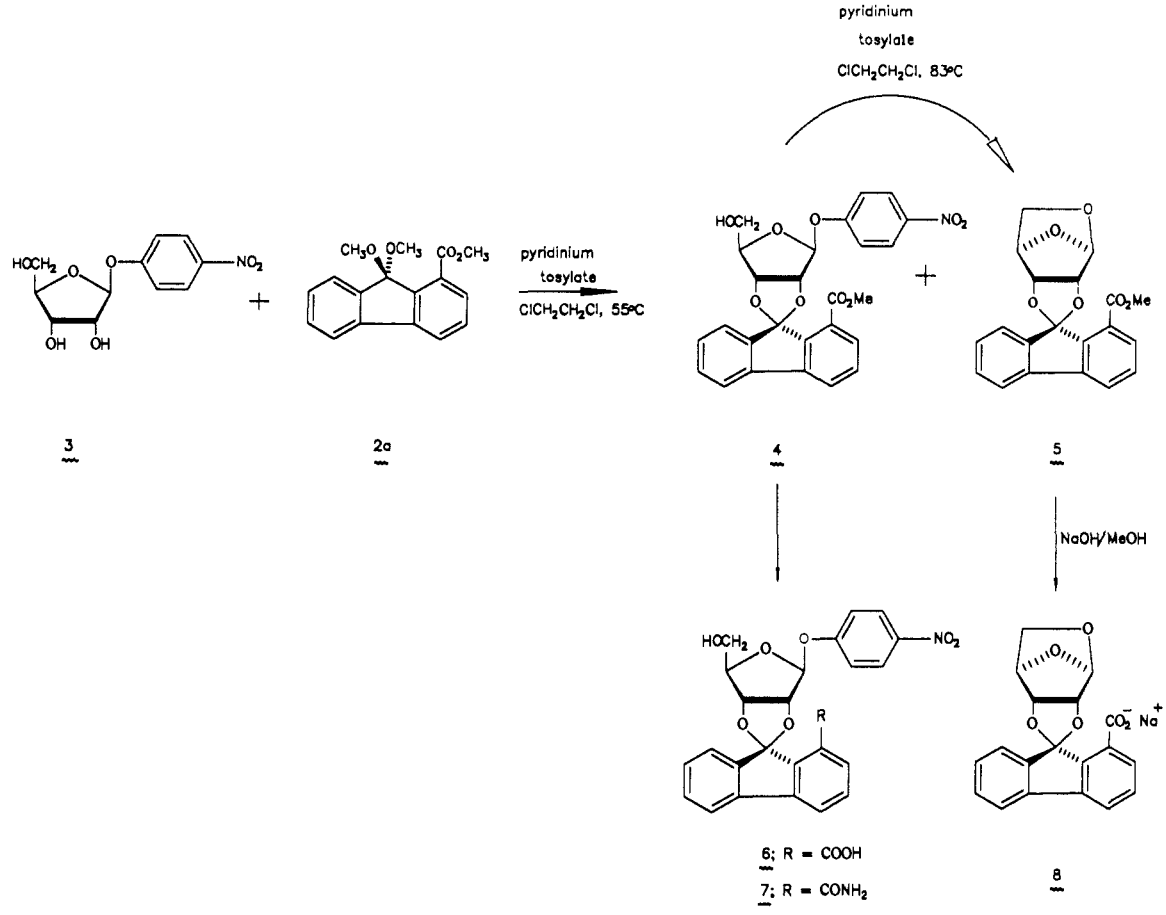


**Scheme V**

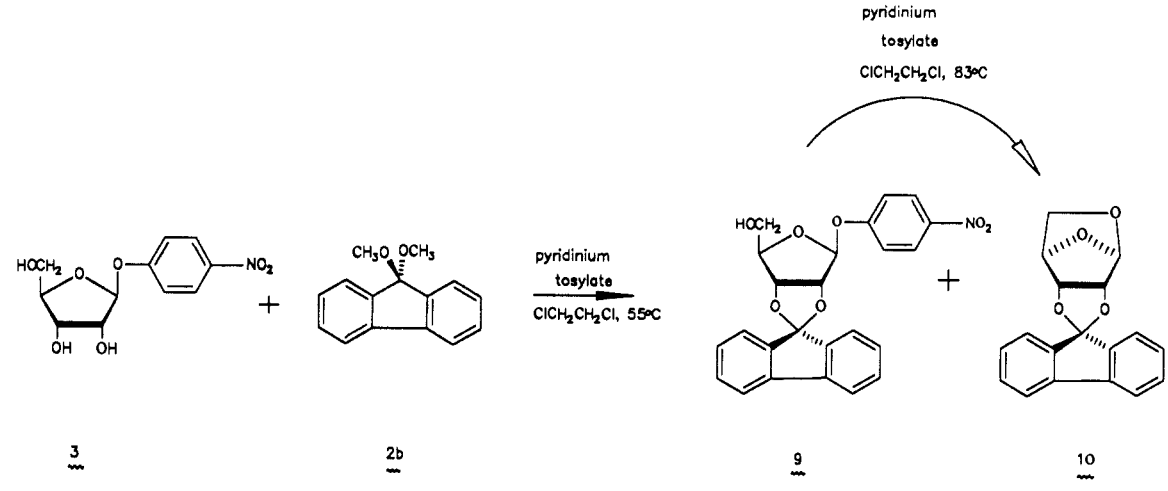


an early indication that the ketal group in **6** was more stable toward hydrolysis than was the ketal group of **2c**. The conversion of ester **4** to amide **7** was accomplished in low yield (5%) by ammonolysis in a bomb reactor. The high temperature (90 °C) required for this ammonolysis was attributed to steric inhibition of tetrahedral intermediate formation in **4** and led to the formation of significant amounts of byproducts. Conversion of ester **5** to sodium carboxylate **8** was accomplished in NaOH/MeOH as used previously. The spiroketalization of **3** with **2b** afforded a mixture of ribosides **9** and **10** (Scheme V), of which formation of only a single diastereomer is possible in each case.

**p$K_a$ Determination.** A p$K_a$ determination of *endo*-acid **6** was accomplished by following the known absorption of benzoates at 242 nm. A plot of pH versus absorbance at 242 nm, obtained by using a solution of **6** (1 mg) in pH 12.9 NaOH solution (50 mL) and titrating with HCl, afforded the titration curve shown

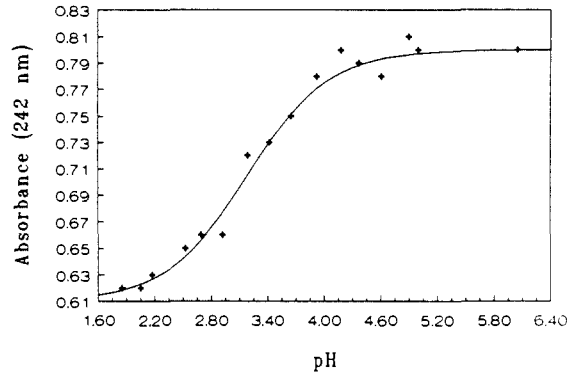


**Figure 4.** Titration of the carboxyl group of *endo*-acid **6** as followed by UV absorbance at 242 nm.

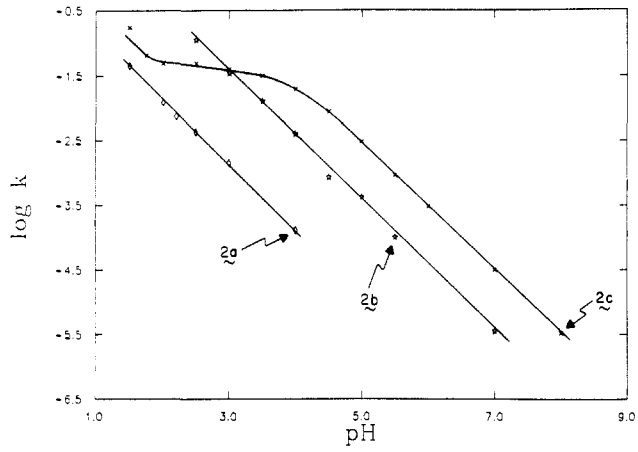


Figure 5. pH–rate profiles for the hydrolyses of ketal ester **2a** (◇), ketal **2b** (☆), and ketal carboxylate **2c** (×) at 30 °C in aqueous solution.

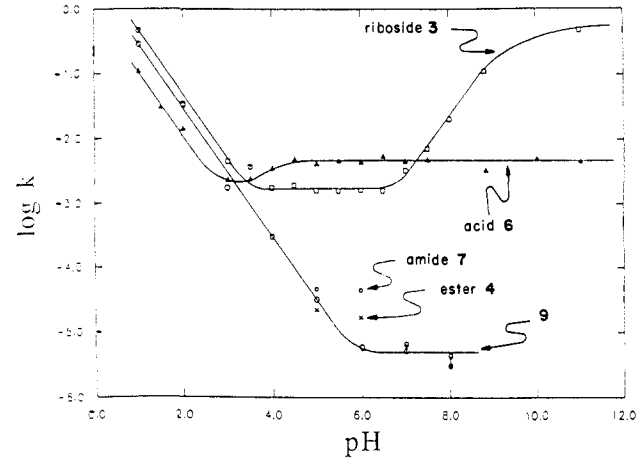


Figure 6. pH–rate profiles for the hydrolyses of *p*-nitrophenyl β-D-ribofuranoside **3** (□), *endo*-ester **4** (×), *endo*-acid **6** (▲), *endo*-amide **7** (△), and protiated **9** at 100 °C in aqueous solution.

in Figure 4, from which a p$K_a$ of 3.2 could be obtained. Over the pH range indicated, the titration was completely reversible. The curve shown in Figure 4 was calculated by the program used for this determination (ENZFITTER, available from Elsevier-BIOSOFT, 68 Hills Road, Cambridge CB2 1LA, U.K.). The measured p$K_a$ of 3.2 in **6** is somewhat unexpected as compared with those of 4.20 for benzoic acid and 3.91 for *o*-toluic acid.[63] Of course, the fluorenone acetal oxygens will serve inductively as electron-withdrawing groups; in addition, the enforced orthogonal orientation of carboxylate and aryl groups in **6** may serve to further lower the p$K_a$ in the same way that the *o*-methyl group of *o*-toluic acid does. The p$K_a$ of benzoic acid is especially temperature insensitive ($d[pK_a]/dT = 0.0003$),[63] so the 70 °C difference between the determinations shown in Figures 4 and 6 would not likely result in a substantial p$K_a$ modulation.

**pH–Rate Studies.** The reaction rates for the hydrolysis of fluorenone ketals **2a–c** were determined at 30 °C by following the increase in absorbance arising from the fluorenone products. pH–rate profiles for these reactions are shown in Figure 5. pH–rate profiles for the formation of *p*-nitrophenol at 100 °C from *endo*-ester **4**, *endo*-acid **6**, *endo*-amide **7**, and protiated reference compound **9** in totally aqueous solution are shown in Figure 6. The curves shown were drawn manually.

## Discussion and Conclusions

*endo*-Acid **6** incorporates several design elements that make it a particularly attractive glycosylase model: (1) the spiro bicyclic linkage places the carboxylate group symmetrically underneath

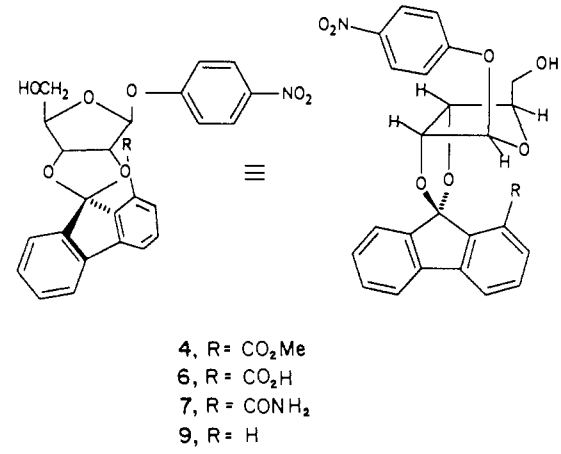


Figure 7. Side perspective view of ribosyl spiro ketal model compounds.

**Scheme VI**

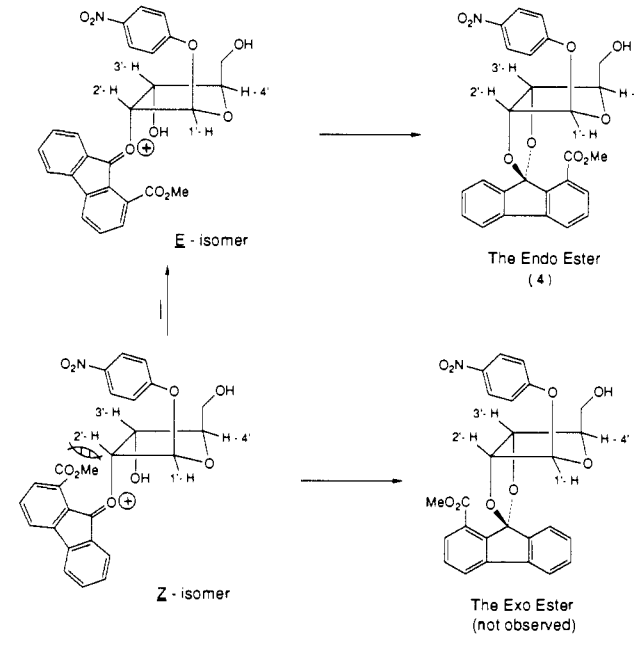


the ribose ring oxygen, enforcing proximity to the syn lone pairs (Figure 7), (2) the rigid fluorene framework prohibits a conformational flexure that would disengage carboxylate and anomeric carbon (or ring oxygen) moieties, and (3) because fluorenone ketals hydrolyze via formally antiaromatic oxonium ion intermediates, they are themselves unusually stable toward hydrolysis.[64]

**Selective Formation of the *endo*-Ester 4.** The spiroketalization reaction between **2a** and **3** is highly stereospecific for the endo product **4**, with none of the exo product observed. We looked quite intensively for even a small amount of the *exo*-ketal, because the corresponding acid would have served as a useful reference compound for kinetic studies. There is, of course, precedence for the stereospecific formation of *endo*-acetals in the reaction of aldehydes with nucleosides,[64] and a similar reasoning may be used to explain the result we have observed. As shown in Scheme VI, the oxocarbonium ion intermediate that closes to the spiro ketal may exist in either *E* or *Z* forms. Because of the instability of oxofluoronium cations, a rigid planarity about the oxocarbonium ion is expected; any deviation from planarity would localize charge on the fluorenone carbon and generate a fluorenium cation, an antiaromatic system. CPK models make it clear that the ester group of the *Z* isomer of the cation will experience a steric repulsion with the ribose 2′-hydrogen, while in the *E* isomer no such repulsive interaction is present. An identical analysis using the isomeric

(63) Albert, A.; Serjeant, E. P. *The Determination of Ionization Constants*, 3rd ed.; Chapman and Hall, Ltd.: New York, 1984.

(64) Bakthavachalam, V.; Lin, L. G.; Cherian, X. M.; Czarnik, A. W. *Carbohydr. Res.* **1987**, *170*, 124.

3′-oxocarbonium ion intermediate yields the same result, with repulsion of the ester in the *Z* isomer with the 3′-hydrogen. Therefore, closure occurs only via the *E* isomer, which can only yield the *endo*-ester **4**.

**Analysis of the X-ray Structure.** The X-ray structure of **8** shown in Figure 3 reveals that the molecule has adopted a geometry minimizing repulsion between lone pairs on the carboxylate oxygens (O5/O6) and the ribose ring oxygen (O3).[65] An envelope flip involving O1–C10–O2 serves as a "pivot" to bring the carboxylate group in and out of the vicinity of C1′/O3, with the ground state in the crystal being away. Such motions may be used to model catalytically productive conformational changes in an ES complex, and one might imagine ways to couple the binding of a species at a receptor in the C8/C2′/C3′ region of the structure to an enhanced catalytic ability of the carboxylate group. As a potential model compound with which to test our ideas concerning lone pair exchange repulsion, one may also envision structural modifications that would further enforce proximity of the carboxylate and ring oxygen groups.

**Analysis of the pH–Rate Profiles. (1) Hydrolysis of Fluorenone Dimethyl Ketals.** As shown in Figure 5, the hydrolyses of both **2a** and **2b** were specific-acid-catalyzed over the pH ranges examined (1.5–4.0 for **2a** and 2.5–7.0 for **2b**). Ketal **2c** additionally demonstrated a nearly pH-independent region from 2.0 to 3.5, which is reasonably attributed to a changing inductive effect caused by carboxyl ionization; nucleophilic participation by carboxylate is not a possibility for geometric reasons. The slower hydrolysis of **2a** as compared to that of **2b** at all pH's likely reflects the electron-withdrawing effect of the ester group in **2a**, which would destabilize the oxocarbonium ion intermediate involved in acid-catalyzed ketal hydrolysis. The midpoint of the plateau region (pH 2–4) for the hydrolysis of **2c**, corresponding to the apparent $pK_a$ for **2c**, occurs at about 3.0 and correlates well with the value of 3.2 obtained for the structurally related *endo*-acid **6**. It therefore seems likely that the carboxylate of **6** is about as available for solvation as is the less sterically encumbered carboxylate of **2c**.

In addition, it is interesting that the specific-acid-catalyzed hydrolysis of **2c** is faster than that of **2b** from pH 4 to 7 by a factor of 150-fold. Inductively, the carboxylate group is electron-*donating* ($\sigma_I^{COO^-} = -0.35$) while the ester group is electron-withdrawing ($\sigma_I^{COOEt} = 0.30$).[66] We choose to compare $\sigma_I$ constants rather than $\sigma_p$ constants because, while an oxocarbonium ion would be conjugated to a group at the fluorenone 1-position, the X-ray structure of **8** shows the carboxylate to be orthogonal to the benzene ring. This structure is consistent with predictions made by molecular mechanics calculations on both **6** and **8**. Therefore, while carboxylate stabilization of the oxocarbonium ion intermediate by a field effect is a mechanistic possibility for the relatively rapid hydrolysis of **6**, the simplest explanation for the observed rate effect is inductive stabilization of the intermediate in a specific-acid-catalyzed pathway. Once again, anchimeric assistance by carboxylate is ruled out for geometric reasons.

**(2) Hydrolysis of *p*-Nitrophenyl β-D-Ribofuranoside.** The hydrolysis of several *p*-nitrophenyl glucosides has been studied by Bruice;[67] however, the pH–rate profile for the hydrolysis of *p*-nitrophenyl β-D-ribofuranoside (**3**) has not been reported previously. As shown in Figure 6, the hydrolysis of riboside **3** (□) demonstrates specific-acid-catalyzed (pH 1–3), pH-independent (4–6.5), and base-catalyzed (7–11) regions. Between pH 4 and 6.5, the reaction is water-catalyzed ("uncatalyzed"). Such pH behavior is also demonstrated by other *p*-nitrophenyl glycosides[67] and permits us to measure the effect of an adjacent catalytic group without complications from other modes of catalysis. For example, it has been shown by Fife that the hydrolysis of electronically symmetrical acetals is not accelerated by an adjacent carboxylate; rather, the presence of a carboxylate group serves to make general-acid catalysis by a different carboxyl group more efficient.[52,54] Finally, the base-catalyzed hydrolysis of $NAD^+$ has been shown by Oppenheimer to result from deprotonation of the 2′-hydroxyl group, which greatly facilitates expulsion of the aglycon;[28] we observe the same leveling effect beginning at pH 11 due to titration of a secondary hydroxyl group.

**(3) Hydrolysis of the Protiated Reference Ketal.** The unsubstituted fluorenone ketal of *p*-nitrophenyl β-D-ribofuranoside, compound **9**, differs structurally from *p*-nitrophenyl β-D-ribofuranoside itself in two important ways: (1) **9** possesses a 2′,3′-ketal group that **3** lacks, and (2) the α-face of the riboside is partially blocked by the fluorene group. The presence of a ketal group on a ribose's 2′,3′-positions has only a small (<15-fold) decelerating effect on the rate of its glycosidic hydrolysis in the pH-independent region. At pH 5 and 100 °C, glycosidic hydrolysis of 2′,3′-isopropylidene-7-methylguanosine is only 13 times slower than that of 7-methylguanosine (R. Sweger, this laboratory; unpublished result). Similarly, the hydrolysis of 2′,3′-isopropylidene-$NAD^+$ is only 4.5 times slower than that of $NAD^+$ at 80 °C and below pH 7.[28] Also, in the pH 1–3 region the specific-acid-catalyzed hydrolysis rate for ketal **9** is only 1.6 times slower that that of the parent riboside **3**. Therefore, while the absence of a hydroxyl group at the 2′-position might have slowed glycosidic hydrolysis by removing it as an internal nucleophile, this is not observed.

However, while **3** switches to the uncatalyzed mechanism by pH 4 (Figure 6), the hydrolysis rate of **9** decreases regularly to pH 6, at which point it becomes pH independent. Data points in this pH-independent region are difficult to obtain with accuracy; after 200 h at 100 °C and pH 7, glycosidic hydrolysis of compound **9** has occurred to only about 8%. At pH's 6, 7, and 8, another reaction begins to consume **9**; the two data points at each of these pH's in Figure 6 represent two determinations for the rate constant at that pH. In fact, the formation of fluorenone (as determined by UV) during these reactions suggests that the rate-limiting step for the release of *p*-nitrophenol from pH 6 to 8 may be hydrolysis of the fluorenone ketal; the resulting product **3** would then hydrolyze quickly. Because we cannot determine which hydrolysis occurs first for these very slow reactions (it is also possible that fluorenone ketal hydrolysis becomes much faster after glycosidic hydrolysis), the data shown should be viewed only as lower limits for the glycosidic hydrolysis reactions at pH 6–8. A better lower limit can be obtained by using more highly activated aglycons; that work is currently in progress.

Thus, the uncatalyzed glycosidic hydrolysis of the fluorenone ketal of *p*-nitrophenyl β-D-ribofuranoside is at least 330 times slower than that of *p*-nitrophenyl β-D-ribofuranoside itself. A rate difference this large cannot be attributed solely to the presence of the ketal group for the reasons given above. Two other structural effects on reactivity seem worthy of consideration. First, the fluorenone ketal may induce the ribose ring to adopt an unreactive conformation. In extreme cases, stereoelectronic effects can modulate the rate of ketal hydrolysis by factors as high as $10^{13}$.[68] We have observed similar, albeit smaller, rate retardations in the hydrolyses of cyclonucleosides.[69] However, the X-ray structure of ketal **10** (unpublished results), which is very similar to that of **8** shown in Figure 3, suggests that the depicted ribose envelope conformation can be readily accommodated by fluorene movement about the O1–C10–O2 pivot. This envelope conformation places one ring oxygen lone pair antiperiplanar to the aglycon oxygen and is expected on stereoelectronic grounds to be optimal for aglycon expulsion.

Instead, we prefer to explain the slow hydrolysis of **9** by invoking hindrance to backside "solvation" of the oxocarbonium ion intermediate. The transition state for substitution at some acetal centers is highly open, involving participation by a preassociated water molecule.[70] On the basis of a complete kinetic isotope study,

(65) Complete details concerning this X-ray structure determination may be found in: Cherian, X. M.; Gallucci, J.; Reid, S. S.; Czarnik, A. W. *Acta Crystallogr.*, in press.
(66) Hine, J. *Structural Effects on Equilibria in Organic Chemistry*; Robert E. Krieger Publishing Company: Huntington, NY, 1981; pp 97–99.
(67) Piskiewicz, D.; Bruice, T. C. *J. Am. Chem. Soc.* **1967**, *89*, 6237.
(68) Briggs, A. J.; Evans, C. M.; Glenn, R.; Kirby, A. J. *J. Chem. Soc., Perkin Trans. 2* **1983**, 1637.
(69) Lin, L.-G.; Bakthavachalam, V.; Cherian, X. M.; Czarnik, A. W. *J. Org. Chem.* **1987**, *52*, 3113.
(70) Sinnott, M. L.; Jencks, W. P. *J. Am. Chem. Soc.* **1980**, *102*, 2026.

Sinnott has concluded that the hydrolysis reactions of aldopyranosyl derivatives in water are truly $S_N1$ with no preassociation of the ultimate nucleophile, in contrast to the behavior of methoxymethyl systems.[30] Therefore, the exclusion of solvent from the backside of the breaking C–O bond of **9** would reasonably slow the hydrolysis reaction only if oxocarbonium ion formation required interaction with solvent on the side opposite the leaving group. It is not possible to build a CPK model of compound **9** that incorporates a water molecule on the $\alpha$-face of the anomeric carbon. We believe ketal **9** provides the first direct experimental verification for the importance of backside solvent participation in an $S_N1$ hydrolysis reaction, first described by Kirby.[71] In addition, these results provide strong evidence that the hydrolysis of $\beta$-D-ribofuranosides *does* require a preassociation nucleophile. It is not unreasonable to conclude that the reactions of aldofuranosyl and aldopyranosyl compounds need not occur via identical transition structures. Further support for this explanation is derived from the rate accelerations observed in the *endo*-ester, -amide, and -acid compounds we have studied.

**(4) Hydrolysis Catalyzed by a Syn-Oriented Carboxylate.** The specific-acid-catalyzed hydrolysis of **6** (Figure 6, $\Delta$) is only 4.3 times slower than that of *p*-nitrophenyl $\beta$-D-ribofuranoside and 2.6 times slower than that of its fluorenone ketal, indicating that the *endo*-COOH group is relatively innocuous with respect to the hydrolysis reaction. It is possible that the only effect of the carboxyl group is to slightly disfavor the productive ribose envelope conformation; it cannot serve as a general-acid catalyst owing to its spatial orientation and to the electronically unsymmetrical nature of the acetal, which guarantees cleavage of the exocyclic C–O bond.

The titration of a catalytically competent species with kinetic $pK_a \leq 3.9$ is observed, which is reasonably attributed to deprotonation of the carboxyl group (thermodynamic $pK_a$ is 3.2). A pH-independent region then follows from pH 4.5 to 11, throughout which the carboxyl group exists totally in the carboxylate form. Because the carboxylate group of **6** is so far from the anomeric center (six bonds), it cannot exert a large polar inductive effect on the glycosidic hydrolysis reaction. Clearly, catalysis in the glycosidic hydrolysis reaction is afforded by the $COO^-$ group, but the magnitude of the acceleration depends on the choice of reference compound. By comparing the pH-independent rates of glycosidic hydrolysis, we calculate that *endo*-acid **6** ($k_1 = 5.1 \times 10^{-3}$ min$^{-1}$) reacts 3.2 times faster than riboside **3** ($k_1 = 1.6 \times 10^{-3}$ min$^{-1}$) and 860 times faster than the fluorenone ketal **9** ($k_1 = 5.9 \times 10^{-6}$ min$^{-1}$).

The comparison of *endo*-acid **6** with ketal **9** (860-fold acceleration by the carboxylate group) seems highly reasonable, given that each contains the 2′,3′-fluorenone ketal group with its resulting (relatively small) rate deceleration and that each is capable of inducing a similar flexure to a less reactive ribose envelope conformation. The comparison is directly analogous to comparing lysozyme with an Asp-52 → Ala-52 mutant enzyme. Such a site-specific mutation would be expected to diminish the catalytic activity because of an inability to solvate the oxonium ion intermediate, a role that Asp-52 accomplishes either electrostatically or covalently. At present, the evidence in total for lysozyme is supportive of nucleophilic participation by carboxylate, and we tend to attribute carboxylate catalysis in **6** to the same effect. As has been pointed out previously, "it is difficult to imagine what sort of conformational restrictions could be strong enough to prevent the oxocarbonium ion–carboxylate pair [from] collapsing to neutralize each other by forming a covalent bond.[72] Our attempts to isolate the *syn*-acylal that would be produced by such a nucleophilic displacement of *p*-nitrophenol by the carboxylate have been inconclusive, but such a compound in equilibrium with its open-chain form in water could give rise to a multitude of products.

The $k_1(\mathbf{6})/k_1(\mathbf{3})$ ratio allows an evaluation of the effectiveness of *syn*-carboxylate catalysis. If we assume that **6** reacts 10 times more slowly than it would if the 2′,3′-ketal group were not present,[73] we calculate that the *endo*-carboxylate gives a rate acceleration of 32 over that afforded by water catalysis. This acceleration is within the range observed for catalysis in intramolecular *anti*-carboxylate model systems and does not denote any special advantage for the syn orientation.

**(5) Hydrolysis Catalyzed by Syn-Oriented Carboxylic Ester and Amide Groups.** At pH 6, the hydrolysis of *endo*-ester **4** (Figure 6, ×) proceeded with $k_1 = 1.8 \times 10^{-5}$ min$^{-1}$ and the hydrolysis of *endo*-amide **7** (Figure 6, $\Delta$) proceeded with $k_1 = 4.5 \times 10^{-5}$ min$^{-1}$. Because of the likelihood of ester or amide hydrolysis at acidic pH and 100 °C, the hydrolyses of **4** and **7** were followed only at two near-neutral pH's (5 and 6). Even under these conditions, we cannot discount the possibility that the observed rate of *p*-nitrophenol formation is due to rate-limiting hydrolysis of the ester or amide group to carboxylate, which would then quickly undergo glycosidic hydrolysis. While the rates might have been expected to vary with pH if this were the case, pH 5–6 could be a nearly pH-independent region for both ester and amide hydrolysis. One argument against this possibility is the fact that the amide would not be expected to hydrolyze more quickly than the ester at these pH's, although ester[74] and amide[75] hydrolyses near pH 5–6 are both exceptionally slow.

Given these provisos, it is certain that the *syn*-amide group of **7** accelerates this reaction but is at least 100 times *less* capable of accelerating the glycosidic hydrolysis reaction than is the *syn*-carboxylate group of **6**. This is as compared to the reported[76] nucleophilicity of amides toward alkyl and aryl esters, which is actually greater than that of carboxylates. Similarly, nucleophilic amide participation in acetal hydrolysis has been shown by Bruice to afford rate accelerations from 50-fold (specific-acid-catalyzed hydrolysis of methyl 2-acetamido-2-deoxy-$\beta$-D-glucopyranoside)[77] to $10^5$-fold (water-catalyzed hydrolyses of nitrophenyl 2-acetamido-2-deoxy-$\beta$-D-glucopyranoside).[67] However, amide **7** does not provide a net acceleration as compared to the uncatalyzed hydrolysis of **3**. At face value, our finding gives support to an electrostatic stabilization function for carboxylate, which should be superior to that of an amide at the same distance. However, it is worth noting that the amide has two hydrogens on the nitrogen, while the carboxylate is unsubstituted at the same position. The partial negative charge on each carboxylate oxygen will create an electrostatic repulsion completely analogous to "steric" repulsion, so this effect must be attenuated to an extent that cannot be quantified. Similarly, the ester group of **4** is expected to be both a poorer nucleophile than carboxylate and less able to stabilize an oxocarbonium ion. Kinetics reveal that the *syn*-ester group of **4** is at least 240 times less capable of accelerating the glycosidic hydrolysis reaction than is the carboxylate group of **6**.

**How These Kinetic Studies Relate to the Mechanism of Nucleoside Glycosylases.** Four different ways have been proposed in which a carboxylate group might accelerate the glycosidic hydrolysis reaction. The preceding discussion of kinetic effects in our model compounds can be distilled into support or lack of support for each.

**(1) Electrostatic Stabilization of an Oxocarbonium Ion like Transition Structure.** Purely electrostatic stabilization as a means of accelerating the formation of oxocarbonium ions in enzyme model systems has been largely discounted on the basis of the work of Loudon.[56] However, the 100-fold enhanced activity of the

(71) Craze, G.-A.; Kirby, A. J. *J. Chem. Soc., Perkin Trans. 2* **1978**, 357.
(72) Reference 33b, p 294. The issue of whether or not such a covalent intermediate could reasonably be formed via an ion-paired transition structure remains a matter of debate.
(73) The factor of 10 here is roughly the deceleration observed in the hydrolyses of 2′,3′-isopropylidene-NAD$^+$ and 7-methylguanosine as compared to those of the free nucleosides. In addition, the specific-acid-catalyzed hydrolysis of **6** is 4.3 times slower than that of **3**.
(74) Guthrie, J. P. *J. Am. Chem. Soc.* **1973**, *95*, 6999.
(75) (a) Kahne, D.; Still, W. C. *J. Am. Chem. Soc.* **1988**, *110*, 7529. (b) Hine, J.; King, R. S.-M.; Midden, W. R.; Sinha, A. *J. Org. Chem.* **1981**, *46*, 3186.
(76) Suh, J.; Yoon, S. S.; Oh, E.; Kang, C.; Lee, E. *Bioorg. Chem.* **1988**, *16*, 245.
(77) Piszkiewicz, D.; Bruice, T. C. *J. Am. Chem. Soc.* **1968**, *90*, 5844.
(78) Unpublished results, A. Moorman and this laboratory.

*endo*-carboxylate **6** as compared to the *endo*-amide **7** nonetheless argues in favor of the electrostatic stabilization mechanism.

**(2) Anchimeric Assistance.** While this seems the most likely explanation for the observed catalysis in lysozyme models, the lack of similar reactivity in *endo*-amide **7** argues against nucleophilic participation by the carboxylate group in **6**. In addition, the fact that the calculated rate acceleration afforded by the syn-oriented carboxylate is not larger than that reported by *anti*-carboxylate model systems disfavors the $S_N2$ mechanism; clearly, however, the role of attack angle as discussed by Houk[59] has not been addressed, nor has the effect of carboxylate on the conformational preference of the ribose ring. On the other hand, if the function of the carboxylate group were to hydrogen-bond to and orient a water molecule for $\alpha$-side attack (or solvation, as proposed by Sinnott and Jencks[70]), the carboxylate (the $pK_a$ of acetic acid is 4.8) would serve as a more effective "general base" than the amide (the $pK_a$ of the conjugate acid of acetamide is −1.4).

**(3) Electrostatic Destabilization of the ES Complex by Binding-Induced Desolvation of the Carboxylate Ion.** Because the apparent $pK_a$ values for carboxylic acids **2c** and **6** are so similar (3 versus 3.2), there can be no unusual hindrance to hydration of the carboxylate group and therefore ground-state desolvation is not a likely mechanism for catalysis in *endo*-acid **6**. It is worth mentioning that the ready solvation of **6** stands in contrast to our explanation of hindered solvation in the hydrolysis of **9**. The presence of a carboxylate ion will push the carboxylate and ribose ring oxygens as far apart as possible, perhaps opening a space for water. In addition, a carboxylate may be solvated via the anti lone pairs, which protrude out from under the ribose ring. Of course, there is a much stronger driving force for solvation of the carboxylate ion than for solvent incorporation into the kind of hydrophobic pocket presumably present on the $\alpha$-face of **9**.

**(4) Lone Pair Exchange Repulsion.** The X-ray structure of **8** shown in Figure 3 clearly indicates a *lack* of significant enforced overlap of carboxylate and ring oxygen lone pair electrons. The degree of freedom remaining in **8** is sufficient to permit an O3–O5 interatomic distance of 3.22 Å,[65] larger than the corresponding distance (2.5–3.0 Å) between the Asp-52 carboxylate oxygen and the ring oxygen of lysozyme's bound substrate.[42] In addition, the lone pairs are not pointing at one another (required for maximal repulsion) but exist in a skew orientation. Most importantly, the corresponding O3–O5 interatomic distance in carboxylate **6** is likely to be even larger, given the additional degrees of freedom. Therefore, lone pair exchange repulsion is also not a likely mechanism for catalysis in *endo*-acid **6**. Structural modifications may be envisioned that would permit the testing of this effect.

## Summary

We have compared the pH-independent rates of glycosidic hydrolysis in a series of four fluorenone ketal derivatives of *p*-nitrophenyl β-D-ribofuranoside with each other and with that of *p*-nitrophenyl β-D-ribofuranoside itself. A syn-oriented carboxylate group clearly affords catalysis in the reaction and is more effective than identically oriented amide and ester groups by factors of at least 100- and 240-fold, respectively. The effect of the carboxylate can be viewed in three different ways: it provides a 3.2-fold acceleration as compared to underivatized *p*-nitrophenyl β-D-ribofuranoside, an approximately 30-fold acceleration when the decelerating effect of the ketal group is considered, and an 860-fold acceleration as compared to the compound that models an Asp-52 → Ala-52 mutant lysozyme. Most strikingly, the hydrolysis of a reference compound with impeded backside solvation of the oxocarbonium ion is very slow and provides a direct experimental verification for the importance of backside solvent participation in an $S_N1$ hydrolysis reaction. These kinetic results do not provide any evidence concerning two potential explanations for the role of carboxylate in acetal hydrolysis: electrostatic destabilization of the ES complex by binding-induced desolvation of the carboxylate ion and lone pair exchange repulsion. The results are consistent with two other proposed carboxylate roles: electrostatic stabilization of an oxocarbonium ion like transition structure and anchimeric assistance by the carboxylate. While the most likely role for carboxylate in acetal hydrolysis is as a nucleophile, the lack of reactivity of the *endo*-amide and unsurprising reactivity of the *endo*-carboxylate more directly support the electrostatic stabilization mechanism.

## Experimental Section

**General.** Melting points were taken on an Electrothermal melting point apparatus and are uncorrected. Microanalyses were carried out at Canadian Microanalytical Service, New Westminster, BC. Mass spectra were obtained by use of a Kratos 30 mass spectrometer. FT-NMR spectra were obtained at 11.75 T (500 MHz) or 7.0 T (300 MHz). UV spectra were obtained on a Hewlett-Packard 8451A diode array spectrophotometer; all wavelength data reported are ±1 nm.

**9,9-Dimethoxy-1-methoxycarbonylfluorene (2a).** 1-Carboxyfluorenone[61] (1.0 g, 4.46 mmol) was stirred in methanol (150 mL) and trimethyl orthoformate (67 mL) at reflux until dissolution. *p*-Toluenesulfonic acid (4.0 g) was added and the solution was refluxed overnight. After cooling, the reaction was neutralized with excess 2 N ammonia in ethanol. The solution was rotary-evaporated to dryness, extracted with chloroform to remove ammonium tosylate, and filtered. The filtrate was rotary-evaporated to dryness and chromatographed on a silica gel column with $CHCl_3$/hexane (9:1) as eluent. Crystallization from hexane gave 9,9-dimethoxy-1-methoxycarbonylfluorene (0.66 g, 52%): mp 72–76 °C; TLC ($CHCl_3$/5% EtOH/5% hexane) $R_f$ 0.66; $^1H$ NMR ($CDCl_3$) δ 3.1 (s, 6 H, $COCH_3$ ketal), 4.0 (s, 3 $COCH_3$ ester), 7.5 (m, 6.3 H, ArH); $^{13}C$ NMR ($CDCl_3$) δ 51.45, 51.86, 96.37, 109.62, 119.91, 122.15, 124.68, 128.21, 128.92, 129.90, 131.42, 139.50, 140.68, 141.23, 141.87, 166.78; EI mass spectrum, *m/e* 284 ($M^+$), 253 ($M^+ - OCH_3$). Anal. Calcd for $C_{17}H_{16}O_4$: C, 71.82; H, 5.67. Found: C, 71.69; H, 5.74.

**9,9-Dimethoxyfluorene (2b)** was prepared according to the literature procedure described in ref 64.

**Sodium 9,9-Dimethoxyfluorene-1-carboxylate (2c).** 9,9-Dimethoxy-1-methoxycarbonylfluorene (**2a**; 0.66 g, 2.32 mmol) was dissolved in methanol (10 mL), and a solution of 25% aqueous NaOH (7.2 mL) was added. The resulting solution was allowed to stand overnight without stirring, which resulted in the formation of **2c** as colorless needles (0.39 g, 57%): $^1H$ NMR ($D_2O$) δ 2.86 (s, 6 H, $OCH_3$), 7.12–7.58 (m, 7 H, ArH); $^{13}C$ NMR ($D_2O$) δ 51.25, 110.21, 119.45, 120.08, 124.01, 125.82, 128.34, 130.66, 130.96, 133.68, 138.36, 139.45, 139.82, 140.37, 176.43. Anal. Calcd for $C_{16}H_{13}O_4Na{\cdot}1.5H_2O$: C, 60.19; H, 5.05; Na, 7.20. Found: C, 60.22; H, 5.08; Na, 7.41.

***p*-Nitrophenyl *endo*-2′,3′-*O*-(1-Methoxycarbonyl-*o*,*o*′-biphenylenemethylidene)ribofuranoside (4).** To a suspension of *p*-nitrophenyl ribofuranoside[62] (**3**; 5.4 g, 20 mmol) in freshly distilled dichloroethane (600 mL) was added 9,9-dimethoxy-1-methoxycarbonylfluorene (**2a**; 5.7 g, 20 mmol) with stirring. Pyridinium tosylate (600 mg, 2.5 mmol) was added, and the temperature was slowly increased to 55 °C over a period of 4 h. After being stirred for 48 h at 55 °C, the reaction mixture was cooled, diluted with dichloroethane, and washed with dilute ammonium hydroxide and with water, and the organic layer was dried over $Na_2SO_4$. Silica gel chromatography eluting with $CHCl_3$/hexane (1:1) provided the crude product, which was further purified by using a preparative TLC plate and eluting with $CHCl_3$/EtOAc (8:2). The band running with $R_f$ 0.45 [silica gel, $CHCl_3$/EtOAc (8:2)] was isolated and recrystallized from $CHCl_3$/hexane to afford a small amount of anhydroriboside **5** (0.25 g, 4%) and **4** (2.0 g, 25% based on unreacted starting material recovered): mp 196–198 °C; $^1H$ NMR [$(CD_3)_2SO$] δ 3.40–3.50 (m, 2 H, 5′-H), 3.94 (s, 3 H, ester $CH_3$), 4.35–4.41 (q, 1 H, OH), 4.98 (t, 1 H, 4′-H), 5.45–5.54 (dd, 2 H, 2′-H, 3′-H), 6.06 (s, 1 H, 1′-H), 7.18–7.22 (d, 2 H, *p*-NP ArH), 7.34–7.92 (m, 7 H, ArH), 8.22–8.26 (d, 2 H, *p*-NP ArH); $^{13}C$ NMR [$(CD_3)_2SO$] δ 13.5, 22.8, 43.8, 47.2, 48.7, 66.4, 76.5, 77.8, 81.7, 83.2, 84.3, 86.9, 88.7, 90.2, 91.3, 92.6, 93.1, 96.5, 97.9, 101.9, 102.9, 104.7, 121.9, 128.3; FAB mass spectrum, *m/e* 492 ($M^+$), 353 ($M^+$ – *p*-nitrophenol). Anal. Calcd for $C_{26}H_{21}NO_9$: C, 63.54; H, 4.31; N, 2.85. Found: C, 63.50; H, 4.29; N, 2.81.

***endo*-2′,3′-*O*-(1-Methoxycarbonyl-*o*,*o*′-biphenylenemethylidene)-1′,5′-cycloribofuranose (5).** A solution of **4** (490 mg, 1 mmol) in dichloroethane (20 mL) was refluxed overnight in the presence of pyridinium tosylate (24 mg, 0.1 mmol). The progress of the reaction was monitored by TLC [$R_f$ 0.5, silica gel, chloroform/ethyl acetate (8:2)]. The reaction mixture was cooled, diluted with dichloroethane, and washed with dilute ammonium hydroxide and with water, and the organic layer was dried over anhydrous $Na_2SO_4$. The crude product was purified by preparative TLC and crystallized from $CHCl_3$/hexane to afford **5**: mp 179–180 °C; $^1H$ NMR [$(CD_3)_2SO$] δ 3.30–3.36 (m, 1 H, 5′-H), 3.43–3.46 (d, 1 H, 5′-H), 3.85 (s, 3 H, ester $CH_3$), 4.70–4.72 (d, 1 H, 4′-H), 4.85–4.86 (d, 1 H, 3′-H), 4.93–4.96 (d, 1 H, 2′-H), 5.58 (s, 1 H, 1′-H), 7.2–7.86 (m, 7 H, ArH); $^{13}C$ NMR [$(CD_3)_2SO$] δ 52.1, 62.5, 76.5, 79.2, 81.2, 98.5, 113.6, 120.4, 121.3, 122.9, 127.0, 128.9, 129.9, 131.2, 132.9, 134.9, 136.8, 140.6, 144.5, 167.4; FAB mass spectrum, *m/e* 353

($M^+$). Anal. Calcd for $C_{20}H_{16}O_6$: C, 68.18; H, 4.58. Found C, 68.08; H, 4.51.

***p*-Nitrophenyl *endo*-2′,3′-*O*-(1-Carboxy-*o*,*o*′-biphenylenemethylidene)ribofuranoside (6).** To a suspension of **4** (10 mg, 0.02 mmol) in ethanol (1 mL) was added a solution of 25% aqueous NaOH (0.5 mL). The reaction mixture became a clear yellow solution, and stirring was continued for an additional hour. The reaction was neutralized with 10% aqueous acetic acid and extracted with EtOAc. The organic layer was washed with water, dried over anhydrous $Na_2SO_4$, and evaporated to dryness. Crystallization from chloroform/hexane gave *endo*-acid **6** in >90% yield: mp 152–154 °C; $^1$H NMR ($CDCl_3$) δ 3.74–3.77 (t, 2 H, 5′-H), 4.83–4.86 (t, 1 H, 4′-H), 5.54 (s, 2 H, 2′-H, 3′-H), 6.13 (s, 1 H, 1′-H), 7.15–7.85 (m, 9 H, ArH), 8.07–8.11 (d, 2 H, *p*-NP ArH); $^{13}$C NMR [$(CH_3)_2CO$] δ 62.1, 82.8, 86.7, 87.6, 106.0, 116.9, 119.9, 121.8, 122.6, 125.1, 128.4, 129.7, 131.0, 132.1, 136.6, 137.0, 141.2, 142.0, 144.1, 161.1, 167.1, 205.0; FAB mass spectrum, *m*/*e* 478 ($M^+$).

***p*-Nitrophenyl *endo*-2′,3′-*O*-(1-Aminocarbonyl-*o*,*o*′-biphenylenemethylidene)ribofuranoside (7).** To a suspension of *endo*-ester **4** (49.1 mg, 0.1 mmol) in ethanol (7 mL) cooled to −70 °C in a steel bomb was added ammonia (ca. 10 mL). After the vessel was sealed, the temperature was slowly increased to 90 °C and the mixture was left overnight. The progress of the reaction was monitored by TLC on silica gel [$R_f$ 0.2, $CHCl_3$/EtOAc (1:1)]. The crude product was purified by preparative TLC using the same solvent system to obtain amide **7** (5%): $^1$H NMR ($CDCl_3$) δ 3.74–3.77 (m, 2 H, 5′-H), 4.10–4.13 (q, 1 H, 5′-OH), 4.70–4.73 (t, 1 H, 4′-H), 5.51 (s, 2 H, 2′-H, 3′-H), 6.10 (s, 1 H, 1′-H), 6.6 (br s, 1 H, $NH_2$), 6.9 (br s, 1 H, $NH_2$), 7.1–7.17 (d, 2 H, *p*-NP ArH), 7.29–7.71 (m, 7 H, ArH), 8.06–8.11 (d, 2 H, *p*-NP ArH); high-resolution FAB mass spectrum, calcd for $C_{25}H_{21}N_2O_8$, 477.1291, measured, 477.1297.

***endo*-2′,3′-*O*-(1-Carboxy-*o*,*o*′-biphenylenemethylidene)-1′,5′-cycloribofuranose, Sodium Salt (8).** A suspension of cyclic *endo*-ester **5** (50 mg, 0.14 mmol) in methanol (3 mL) was stirred for 3 h, followed by gentle warming for 5 min to obtain a clear solution. This solution was cooled to room temperature, sodium hydroxide (0.5 mL, 25% aqueous solution) was added, and the solution was left overnight without stirring. The fine crystalline solid was filtered to afford **8** (30 mg, 59%): $^1$H NMR [$(CD_3)_2SO$] δ 3.39–3.43 (m, 2 H, 5′-H), 4.61–4.64 (d, 1 H, 4′-H), 4.85–4.93 (dd, 2 H, 2′-H, 3′-H), 5.56 (s, 1 H, 1′-H), 6.92–7.67 (m, 7 H, ArH); $^{13}$C NMR [$(CD_3)_2SO$] δ 62.5, 76.9, 79.0, 81.0, 98.6, 114.4, 116.6, 119.7, 122.5, 125.8, 127.9, 129.2, 130.0, 131.9, 137.8, 139.5, 144.5, 145.4, 172.1; FAB mass spectrum, *m*/*e* 361 ($M^+$). The structure assignment was further confirmed by X-ray analysis, shown in Figure 3.

***p*-Nitrophenyl 2′,3′-*O*-(*o*,*o*′-Biphenylenemethylidene)ribofuranoside (9).** To a suspension of *p*-nitrophenyl ribofuranoside (**3**; 900 mg, 3.3 mmol) in freshly distilled dichloroethane (150 mL) was added 9,9-dimethoxyfluorene (**2b**; 750 mg, 3.3 mmol) with stirring. Pyridinium tosylate (83 mg, 0.33 mmol) was added; then the temperature was slowly increased to 65 °C over a period of 4 h, and the solution was refluxed for 48 h. The reaction mixture was cooled, diluted with dichloroethane, and washed with dilute ammonium hydroxide and with water, and the organic layer was dried over anhydrous $Na_2SO_4$. The crude product was purified by chromatography on silica gel [$CHCl_3$/hexane (2:3)] followed by crystallization from $CHCl_3$/methanol (1:1) to afford **9** (370 mg, 26%): mp 112–113 °C; $^1$H NMR [$(CD_3)_2SO$] δ 3.42–3.55 (m, 2 H, 5′-H), 4.40–4.46 (q, 1 H, OH), 4.95–5.15 (t, 1 H, 4′-H), 5.46–5.50 (m, 2 H, 2′-H, 3′-H), 6.25 (s, 1 H, 1′-H), 7.25–7.77 (m, 10 H, ArH), 8.22 (d, 2 H, ArH); $^{13}$C NMR [$(CD_3)_2SO$] δ 61.7, 83.0, 86.1, 88.3, 105.4, 115.3, 116.8, 120.2, 120.4, 123.4, 124.4, 125.6, 128.5, 130.2, 131.1, 138.1, 139.5, 141.1, 141.8, 143.8, 160.7; FAB mass spectrum, *m*/*e* 434 ($M^+$), 295. ($M^+$ − *p*-nitrophenol). Anal. Calcd for $C_{24}H_{19}NO_7$: C, 66.50; H, 4.42; N, 3.23. Found: C, 66.41; H, 4.40; N, 3.23.

**2′,3′-*O*-(*o*,*o*′-Biphenylenemethylidene)-1′,5′-cycloribofuranose (10)** was another product obtained from the chromatography, in 20% yield. Crystallization from $CHCl_3$/methanol (1:1) gave a colorless solid: mp 216–217 °C; $^1$H NMR [$(CD_3)_2SO$] δ 3.35–3.39 (m, 1 H, 5′-H), 3.43–3.46 (d, 1 H, 5′-H), 4.72–4.75 (d, 1 H, 4′-H), 4.97–5.01 (m, 2 H, 2′-H, 3′-H), 5.70 (s, 1 H, 1′-H), 7.24–7.71 (m, 8 H, ArH); $^{13}$C NMR [$(CD_3)_2SO$] δ 62.4, 77.4, 79.8, 81.6, 99.1, 113.8, 120.0, 120.3, 122.9, 124.8, 128.2, 128.4, 129.8, 130.9, 138.0, 139.5, 141.2, 144.9; FAB mass spectrum, *m*/*e* 295 ($M^+$). Anal. Calcd for $C_{18}H_{14}O_4$: C, 73.46; H, 4.79. Found: C, 73.21, H, 4.60.

**Kinetic Measurements.** The following buffers (50 mM) were used for all kinetics studies: pH 1–2, HCl/KCl; pH 3–5.5, potassium phthalate; pH 6–7.5, potassium phosphate; pH 8.8–10, sodium borate; pH 11, CAPS/NaOH. The hydrolysis of fluorenone ketals was followed by using solutions of **2a** ($8.9 \times 10^{-5}$ M), **2b** ($1.1 \times 10^{-4}$ M), or **2c** ($4.5 \times 10^{-4}$ M) in the appropriate buffer equilibrated at 30 °C. The increase in absorbance at 278 nm (**2a**), 328 nm (**2b**), or 336 nm (**2c**) was used to monitor the formation of the respective fluorenones. The hydrolyses of *p*-nitrophenyl ribofuranoside and its derivatives were accomplished as follows. A solution of the appropriate buffer (60 mL) was equilibrated at 100 ± 0.5 °C overnight; then a solution of the *p*-nitrophenyl ribofuranoside derivative (2 mg) in hot dioxane (1 mL) was added. Aliquots were withdrawn at various time intervals, cooled to room temperature, and diluted with an equal volume of 1.0 M pH 9 buffer to effect the complete deprotonation of *p*-nitrophenol (necessary for pH <8 reactions). The increase in absorbance at 404 nm was used to monitor the formation of *p*-nitrophenolate. Because of the very slow reaction rates for **4**, **7**, and **9** at pH 5–8, these reactions were not followed to completion; $A_\infty$ values were calculated on the basis of the known concentration of starting material. The determination of first-order rate constants was accomplished by using the computer program LSTSQ, available from Serena Software, 489 Serena Lane, Bloomington, IN 47401.

**Acknowledgment.** The financial support of the American Cancer Society is acknowledged with gratitude. We acknowledge the technical assistance of Robert Hrouda for the preparation of ketal **2a** on a large scale. FT-NMR spectra were obtained by using equipment funded in part by NIH Grant 1 S10 RR01458-01A1. One of us (X.M.C.) thanks the Government of India for providing a National Fellowship. A.W.C. thanks the A. P. Sloan and Dreyfus Foundations for support in the form of fellowships and Eli Lilly and Co. and Merck for support in the form of granteeships.